UNCLASSIFIED Copy No. 8
CONFIDENTIAL
RM No. L8K01

3 1176 00035 5785

NACA RM No. L8K01

NACA

RESEARCH MEMORANDUM

EFFECT OF WING SWEEP, TAPER, AND THICKNESS RATIO ON THE TRANSONIC DRAG CHARACTERISTICS OF WING-BODY COMBINATIONS

By

Jim Rogers Thompson and Charles W. Mathews

Langley Aeronautical Laboratory
Langley Field, Va.

CLASSIFICATION CANCELLED CLASSIFIED DOCUMENT

Author: NACA RM 52403 Date 8/1/57

By JNH 9/8/54 See

This document contains classified information affecting the National Defense of the United States within the meaning of the Espionage Act, USC 50:31 and 32. Its transmission or the revelation of its contents in any manner to an unauthorized person is prohibited by law. Information so classified may be imparted only to persons in the military and naval services of the United States, appropriate civilian officers and employees of the Federal Government who have a legitimate interest therein, and to United States citizens of known loyalty and discretion who of necessity must be informed thereof.

NATIONAL ADVISORY COMMITTEE
FOR AERONAUTICS

WASHINGTON

December 31, 1948

UNCLASSIFIED

CONFIDENTIAL

UNCLASSIFIED

NATIONAL ADVISORY COMMITTEE FOR AERONAUTICS

RESEARCH MEMORANDUM

EFFECT OF WING SWEEP, TAPER, AND THICKNESS RATIO ON THE TRANSONIC DRAG CHARACTERISTICS OF WING-BODY COMBINATIONS

By Jim Rogers Thompson and Charles W. Mathews

SUMMARY

As part of an investigation by the National Advisory Committee for Aeronautics of the aerodynamic characteristics of possible transonic and supersonic airplane arrangements, the transonic drag characteristics of a series of wing-body combinations and their component parts are being measured by the free-fall method. Configurations so far investigated have consisted of wings of various sweeps and thickness ratios mounted on identical bodies of fineness ratio 12. Results for three configurations - two having untapered 35° sweptback wings with thickness ratios of 0.09 and 0.12, and one having a 35° sweptback wing tapered 1.467:1 with thickness ratio of 0.12 - are reported herein and are compared with previous results and with theoretical calculations to show the effects of wing sweep angle, taper, and thickness ratio on the transonic drag characteristics of wing-body combinations.

For all the configurations so far investigated, either reduction of wing thickness ratio or increase in the sweep angle produced large reductions in the wing and total drag at supersonic speeds and delayed the occurrence of the drag rise to higher Mach numbers.

The drag of the body-tail combination of the configurations having untapered wings was somewhat increased by either reduction of wing sweepback angle or increase in thickness ratio but remained lower at supersonic speeds than that of an identical body-tail combination tested without wings. The drag of the body-tail combination in the presence of either a sweptforward tapered wing or a sweptback tapered wing was considerably increased over that of the body-tail combination without wings. The wing drags were not appreciably affected, however, either by taper or by the sign at the sweep angle.

The results obtained for the 35° swept wings were not consistent with those predicted by linearized theory for swept wings of finite span (NACA TN No. 1319) but correlated satisfactorily with results for unswept

 UNCLASSIFIED

wings when plotted in the form $\frac{C_D}{\cos^3\Lambda(t/c)^2}$ against $M\sqrt{\cos\Lambda}$.

Correlation for the 45° sweptback wing on this basis was also satisfactory except above a Mach number of 1.02. The presence of the body reduced the Mach number at which the abrupt rise in wing drag occurred by an amount approximately equal to the difference between the estimated local Mach number on the body at the wing root and the flight Mach number.

INTRODUCTION

As part of a general study by the NACA of aerodynamic shapes at transonic and supersonic speeds, the Flight Research Division of the Langley Laboratory is investigating the transonic drag characteristics of wings, bodies, and wing-body combinations by the free-fall method. Previous results have confirmed the low-drag potentialities of bodies of high fineness ratio and swept wings; however, when such low-drag components were combined, important interference effects on the drag were found. The free-fall tests of wing-body combinations have been extended to obtain further understanding of these interference effects and, at the same time, to determine the effects of large changes in basic design variables on the drag.

Wing-body combinations so far investigated have consisted of swept wings mounted on identical bodies of fineness ratio 12 having small boom-mounted stabilizing tail surfaces. Details of these configurations and the model numbers by which they are designated in this paper are shown in the following table:

Model	Sweep		Aspect ratio (based on total wing area)	Taper ratio (center chord to tip chord)	Airfoil (NACA) (perpendicular to quarter chord)	Wing location (from max. body diam.)	Reference
	Quarter chord (deg)	Midchord (deg)					
1	(a)	(a)	(a)	(a)	(a)	(a)	1
2	45	45	4.1	1:1	65-009	Ahead	2
3	45	45	4.1	1:1	65-009	Behind	3
4	-30	-33.7	4.0	2:1	65-012	Behind	4
5	35	35	4.8	1:1	65-009	Behind	Present paper
6	35	35	4.8	1:1	65_1-012	Behind	Present paper
7	35	32.9	4.8	1.467:1	65_1-012	Behind	Present paper

[a] Body-tail arrangement tested without wings.

The transonic drag characteristics for models 5, 6, and 7 are presented herein and are compared with results previously reported to provide some information on the effects of wing sweep angle, thickness ratio, and taper ratio on the drag of wing-body combinations and their component parts at transonic and low supersonic speeds.

TESTS AND RESULTS

Results obtained from the tests of models 1 to 4 and descriptions of these models were reported in references 1 to 4; therefore, this section is limited to tests and results for models 5 to 7.

Models.- A drawing showing details and dimensions of models 5 to 7 is presented as figure 1, and photographs of models 5 and 7 are presented as figure 2. The body-tail combinations of the models were identical and differed from those of models 1 to 4 only by the addition of an airspeed head mounted on a small, cylindrical boom extended from the nose of the body. Coordinates of the body contour are presented in table I. The wings of models 5 to 7 were swept back 35° (measured at the quarter-chord line) and had NACA 65-series sections in planes perpendicular to the quarter-chord line. The wings differed in taper ratio and thickness; models 5 and 6 had untapered wings with thickness ratios of 0.09 and 0.12, respectively, and model 7 had a 1.467:1 tapered wing with a thickness ratio of 0.12.

The wing of each model was located on the body so that the intersection of the midchord line with the body surface was approximately 15 inches to the rear of the body maximum diameter. This wing position is identical with that of model 3 and about 3 inches ahead of the wing position for model 4. The wing and tail surfaces were mounted on separate drag balances within the body and entered the body through rectangular slots slightly wider than the maximum thickness of the airfoil. The slots at the wing-body juncture were filled with wooden blocks mounted on the wing at the root and shaped to preserve the body contour. Small clearances were provided so that these filler blocks did not rub against the sides of the slots as the wing balance deflected under drag load.

Measurements.- Measurement of the desired quantities was accomplished as in previous free-fall tests (references 1 to 4) through use of the NACA radio-telemetering system and radar and phototheodolite equipment. The following quantities were recorded for each model at two separate ground stations by use of the telemetering system:

(1) The longitudinal force exerted on the body by the wing as measured by a spring balance

(2) The longitudinal force exerted on the body by the tail surfaces as measured by a spring balance

[redacted]

(3) The total retardation of the model as measured by three longitudinal accelerometers (usable ranges: 0 to 0.1, 0 to 0.5, and 0.4 to 1.0g, respectively)

(4) Static pressure at the airspeed head as measured by three aneroid cells (usable ranges: 275 to 875, 700 to 1250, and 1200 to 2150 lb/sq ft abs., respectively)

(5) Total pressure at the airspeed head as measured by four aneroid cells (usable ranges: 275 to 1275, 1200 to 2400, 2250 to 3750, and 3600 to 5600 lb/sq ft abs., respectively)

Precision of measurements.- The estimated maximum uncertainties of the drag parameters presented herein for models 5 to 7 are given in table II for several Mach numbers. The values correspond to a maximum uncertainty in a telemetered quantity of ±1 percent of the full range of the instrument. Considerable evidence has been obtained which indicates that the 1-percent value is a reasonable estimate of the over-all accuracy of the telemetering system.

The uncertainties given in the table for the total and body-tail-combination drag parameters are considerably smaller than similar values quoted in references 1 to 4 due to the use of improved instrumentation recently developed by the Langley Instrument Research Division. This improved instrumentation replaces the single longitudinal accelerometer used previously with several accelerometers having much smaller and slightly overlapping ranges with the result that the uncertainty in the total retardation measured by each accelerometer is reduced in proportion to the ratio of the range of each accelerometer to the total range of retardation required. The ranges of the accelerometers used in the present tests are given in the section entitled "Measurements." In order that only one telemeter channel will be required for the several accelerometers, the indication of each was sampled about 5 times per second through use of mechanical switching equipment. A similar system was used to measure the total and static pressures at the airspeed head.

The Mach numbers determined from the true airspeed-temperature data are considered to be uncertain within ±0.01. As the values of Mach number are used to compute drag coefficients from D/F_p ratios, the percentage uncertainties shown in table II for the drag coefficients are somewhat greater than those shown for the D/F_p ratios.

Values of maximum uncertainty given in table II for the body-tail combination correspond to the sum of the maximum uncertainties in the measured wing and total drags since the drag of the body-tail combination was obtained as the difference between these quantities. The most probable value of the uncertainty for this quantity would be somewhat less than the values quoted.

[redacted]

Reduction of data.- The data were reduced to variations with Mach number of D/Fp ratios and drag coefficients for the complete models and their component parts by use of the atmospheric conditions measured at the time of the tests and the relations

$$M = \frac{V}{49.04\sqrt{T}}$$

and

$$C_{D_F} = \frac{D/Fp}{\gamma/2M^2}$$

where

M	Mach number
V	true airspeed (ground velocity plus wind), feet per second
p	atmospheric pressure, pounds per square foot abs.
T	free-air temperature, degrees Rankine
D	drag, pounds
F	frontal area, square feet
γ	ratio of specific heats of air (1.4)

The drag coefficients for the wings and tail surfaces were based on the areas outside of the body and tail boom, respectively.

No radar and phototheodolite data other than the release conditions were obtained for model 6, and the variations of ground velocity and altitude during its fall were computed by successive integration of vector sums of gravitational acceleration and the directed retardation measured by the longitudinal accelerometers. Excellent agreement between the ground velocity and altitude determined in this manner and by the radar and phototheodolite equipment was obtained for models 5 and 7 and in previous tests (references 1 to 5). The tail drag measured for model 5 is considered to be unreliable and is, therefore, not presented herein.

Results.- The results obtained in the free-fall tests of models 5 to 7 are presented in figure 3 as curves showing the variation of

[redacted]

D/Fp ratio with Mach number for each complete model. In order to illustrate the relative importance of each component with regard to drag contribution, the division of the total drag among the component parts is shown in the figures; approximate percentage contributions at low supersonic speeds are given in the following table:

	Model 5	Model 6	Model 7
Wing	58	66	63
Body-tail combination	42	34	37
Tail	--	8	9

The measurements of total and static pressures at the airspeed head for models 5 to 7 were made for use in other tests and will not be reported herein. Results of pressure measurements on model 5 have been reported in reference 6 and the results for models 6 and 7 were similar. It may be noted, however, that within the estimated uncertainties of the pressure measurements the Mach numbers determined from the airspeed head agreed with the Mach numbers determined from the ground velocity-wind-temperature data which are used throughout this paper.

DISCUSSION

The results for models 5 to 7 which were presented in figure 3 are compared in figures 4 to 9 with similar results for the configurations which have been previously tested. Details of each configuration and the reference from which the data were taken are shown in tabular form at the top of each figure. The aspect ratios given in the figures are based on the over-all span and wing area (including that within the body), and the sweep angles are measured from the line of maximum thickness of the wings. The transonic drag characteristics of each component are discussed separately.

Wing drags - effect of sweepback and thickness.- The measured variations of drag coefficient with Mach number for the untapered wings of models 3, 5, and 6 are compared in figure 4. It is immediately apparent that reduction of the thickness ratio and/or increase in the angle of sweepback greatly reduce the wing drag at supersonic speeds and delay the occurrence of the drag rise to higher Mach numbers.

Included in figure 4 are curves showing the variation of pressure drag coefficient with Mach number for the sweptback wings as computed from the linearized theory presented by Harmon and Swanson in reference 7.

The computations were made for circular-arc airfoils and for values of aspect ratio corresponding to those of the tested wings based on the exposed areas and spans. It is apparent that for the 45° sweptback wing (model 3) the measured drag is of the same order of magnitude as that predicted by the theory if a reasonable value is assumed for the skin-friction drag coefficient. For the 35° sweptback wings (models 5 and 6), however, the agreement is unsatisfactory; the measured values are approximately constant at supersonic speeds, while the theory predicts a steeply rising curve. Reference 3 shows that the drag of a wing similar to that of model 3 mounted through open slots at the rear of a cylindrical body did not rise abruptly near the speed of sound but increased gradually with Mach number, attaining a value at $M = 1.24$ of the same order as that measured for the wing of model 3. Thus, it is evident that the wing drag was affected near the speed of sound by the wing mounting and body shape. It does not appear likely, however, that these effects or the use of sharp-nosed airfoils for the theoretical computation could account for all of the discrepancy between the measured and predicted results for the 35° sweptback wings.

In view of the urgent need for a method for predicting the drag characteristics of swept wings in wing-body combinations, an attempt was made to correlate the limited results presented in figure 4 with results for unswept airfoils tested on cylindrical bodies (reference 8) according to the simple theory for infinite yawed wings. The theory, which has been described in many German reports, leads to the result that the pressure drag coefficient based on plan area C_{D_p} for an unswept wing is related to the pressure drag coefficient $C_{D_{p_\Lambda}}$ of a wing with sweepback Λ having the same thickness ratio normal to the leading edge by

$$C_{D_p} = \frac{C_{D_{p_\Lambda}}}{\cos^3 \Lambda}$$

at $M \cos \Lambda$ where M is the flight Mach number.

German investigators found that much more satisfactory correlation of measured drag characteristics of a family of swept wings was obtained if the data are correlated at $M\sqrt{\cos \Lambda}$ rather than $M \cos \Lambda$. This result was also found to apply to the results presented herein. The effect of this modification is roughly equivalent to assuming that the sweepback is only half as effective in delaying the Mach number at which the drag rise occurs as the theory for infinite yawed wings indicates. The experimental results of figure 4 and reference 8 reduced according to the modified relations (assuming a skin-friction drag coefficient

[redacted]

of 0.005) are presented in figure 5. As reference 8 shows that for unswept airfoils of 9- and 12-percent thickness at low supersonic speeds the pressure drag coefficient C_{D_p} is proportional to the square of the thickness ratio and as a similar result is obtained in supersonic wing theory, the results shown in figure 5 are corrected to a thickness ratio t/c of 0.09 by use of the factor $\left(\frac{t/c}{0.09}\right)^2$.

The results shown in figure 5 divide into two similar groups; the unswept airfoils mounted on cylindrical bodies, falling together (approximately within the accuracy of the Mach number measurement, ±0.01) and the swept airfoils mounted on "streamline" bodies, falling together about $0.07\ M\sqrt{\cos \Lambda}$ lower. In general, the shape of all the curves is similar; however, the 45° sweptback wing does not show the relatively sharp break after the abrupt drag rise evidenced by the others and attains a lower value at the higher values of $M\sqrt{\cos \Lambda}$.

The earlier drag rise of the swept wings mounted behind the maximum diameter of fineness-ratio-12 bodies compared with those for the unswept airfoil mounted on cylindrical bodies appears to result from the presence of the streamline body. It is estimated from the incompressible pressure distribution about the fineness-ratio-12 body (corrected by the method of Lees, reference 9) that the local Mach number in the region of the wing-fuselage juncture is about 0.05 greater than the free-stream Mach number at the high subsonic speeds at which the wing drag rises occurred. As both theory and experiment have shown that for a swept wing at transonic speeds the pressure drag is concentrated near the wing root, it appears reasonable that the wing drag is chiefly dependent upon the local Mach number in the region near the wing root and the drag rise would occur when this local Mach number reached the value of free-stream Mach number at which the drag rise occurred for a similar airfoil mounted on a cylindrical body. The incremental Mach number estimated (0.05) is of the same order as the increment shown by the experimental data of figure 5.

As no reliable data are available on the skin friction at transonic speeds, a value of 0.005 (based on plan area) was assumed for all the wings in preparing figure 5. However, most wind-tunnel tests at subsonic speeds have shown somewhat lower skin-friction drag coefficients for swept wings than for unswept wings. Except for the 45° sweptback wing of model 3, the pressure drags for the wings considered herein are large in comparison to the assumed friction drags and, thus, the uncertainty in the friction drag does not significantly affect the data presented. For the wing of model 3 the pressure drag is of the same order as the friction drag, and as a large magnification is introduced by the $\cos^3 45°$ factor, the data presented are significantly affected by the assumed friction drag coefficient. An unreasonably low value of the friction

drag coefficient would be required to account for all of the discrepancy between the 45° and 35° sweptback wings, however.

The abscissa of figure 5 does not include a correction for the effect of thickness ratio and, therefore, the drag rise for the thinner wings should appear in this figure at slightly higher Mach numbers than the drag rises for otherwise comparable wings. The data shown in figure 5 are consistent with this statement. It is apparent that the parameters satisfactorily correlate the experimental results for the swept wings considered except for the 45° sweptback wing above the drag rise. In this case the discrepancy is somewhat greater than the estimated maximum uncertainties in the experimental measurements and the assumed friction drag.

It therefore appears that a useful estimate of the drag of a swept wing mounted on a fuselage can be obtained from data for a similar unswept wing by correcting the drag coefficient in proportion to the cube of the cosine of the sweep angle and the square of the thickness ratio and by correcting the Mach number in proportion to the square root of the cosine of the sweep angle. The effect of the fuselage on the wing drag is included by shifting the drag curve thus derived by an amount equal to the incremental Mach number in the region of the wing root. This result is of course strictly applicable only to the investigated configurations having $\Lambda \approx 35°$ though it provides a satisfactory estimate for the configuration having the 45° sweptback wing until the top of the drag rise is reached ($M\sqrt{\cos \Lambda} \approx 0.90$, $M \approx 1.02$). In the absence of experimental data, the method should provide a useful first approximation to the wing drag for wing-body combinations similar to those investigated.

Wing drags - effect of sweepforward and taper.- The measured variations of drag coefficient with Mach number for the wings of models 4, 6, and 7 are compared in figure 6. Increasing the taper of the sweptback wing from 1:1 to 1.467:1 (models 6 and 7) increased the drag at low supersonic speeds by about 5 percent. However, increasing the taper from 1:1 to 2:1 and sweeping the wing forward (models 6 and 4) did not change the wing drag at low supersonic speeds but delayed the occurrence of the abrupt drag rise by about 0.02 Mach number. Both of these differences are only slightly greater than the estimated maximum uncertainties of the measurements. It is evident that, at least for the wings investigated (sweep $\approx \pm 35°$, thickness ratio 0.12, taper ratio 1:1, 1.467:1, and 2:1), use of sweepforward or sweepback or variation of the taper ratio have little effect on the transonic drag characteristics of the wing. As the drag of a comparable unswept wing near the speed of sound would be about twice the values shown in figure 6, it appears that sweepforward and sweepback are almost equally effective means for reducing the wing drag.

As both the Mach numbers at which the drag rise occurs and the drag at low supersonic speeds measured for the tapered wings of models 4

and 7 agree closely with the results for the untapered wing of model 6, it is evident that the method presented herein for predicting the effect of a fuselage on the wing drag at transonic speeds applies equally well to sweptforward or tapered wings.

Tail drags.- The variations of tail drag coefficient with Mach number measured for models 6 and 7 are compared in figure 7 with results for the identical tails of models previously tested. The results for the tails of models 2, 3, 6, and 7 and of the fineness-ratio-6 body without wings (reference 5) differ by amounts only slightly greater than the estimated maximum uncertainty of the measurements. Although some differences might be expected in the tail drags of the different configurations, no definite trends are evident in these data.

Body-tail-combination drags.- Variations of drag coefficient with Mach number for the identical body-tail combinations of the investigated configurations are compared in figure 8. The drag coefficients are based on the body frontal area and were computed by subtracting the measured wing drag from the measured total drag for each configuration. The data thus contain the interference effects of the wing on the body-tail combination. The comparison is based on the drag of the body-tail combinations rather than the drag of the bodies as reliable measurements of the tail drag are available only for 3 of the 6 models compared. The average drag contributed by the tail is shown in figure 8 by the lower curve. All of the tail drag data of figure 7 fall within the cross-hatched band.

Examination of figure 8 shows that the drag of the body-tail combinations having sweptback untapered wings (models 3, 5, and 6) is lower at supersonic speeds than that of the identical body-tail combination tested without wings (model 1) although the drag rise occurs at a lower Mach number for the models having 35° sweptback wings (models 5 and 6). Thus, the favorable interference effect on the body drag at supersonic speeds due to location of an untapered, sweptback wing behind the maximum body diameter (reported in reference 3) is confirmed. Reduction of the sweepback angle from 45° to 35° (models 3 and 5 or 6) resulted in an unfavorable interference effect just below the speed of sound. At the higher supersonic speeds investigated, the favorable interference effects for models 5 and 6 were of the same order of magnitude as those found for model 3, however. The magnitude of this favorable interference effect is somewhat greater than the estimated maximum uncertainty of the measurements.

Comparison of results for model 6 with those for model 7 in figure 8 shows that changing the taper of the sweptback wing from 1:1 to 1.467:1 increased the drag of the body-tail combination by about 45 percent near the speed of sound. As the drag of the body-tail combination of model 4 (sweptforward wing) is of the same order of magnitude below the speed of sound as that of model 7, it appears that a large unfavorable interference effect of a tapered wing on the drag of the body-tail combination exists for the sweptforward configuration as well as for the sweptback configuration. Just above the speed of sound, however, the drag of the body-tail

combination of model 4 was about 17 percent greater than that of model 7. As the wing of model 4 was tapered 2:1 while that of model 7 was tapered 1.467:1, it is not definitely established whether the higher drags of model 4 above the speed of sound result from the effect of taper or from the sign of the sweep angle.

Total drags.- The measured variations of total drag coefficient with Mach number for models 1 and 3 to 7 are compared in figure 9. The coefficients were based on the body frontal area as that quantity was the same for all the models. It is apparent from figure 9 that either reducing the wing thickness ratio at constant sweep (models 6 and 5) or increasing the wing sweep for a constant thickness ratio (models 5 and 3) considerably reduced the over-all drag at supersonic speeds, reduced the abruptness of the drag rise, and delayed the occurrence of the drag rise to higher Mach numbers. For the models having sweptback wings, the maximum value of the total drag coefficient occurs at successively higher Mach numbers as the wing thickness ratio is reduced or as the sweep angle is increased.

The drag per unit of total frontal area for model 3 is less than that of model 1 at Mach numbers below 1.17, the difference amounting to about 30 percent near the speed of sound. For models 4 to 7, however, the increased wing drag resulting from reduction of the sweep angle and increase of the thickness ratio causes the total drag per unit of total frontal area to be considerably greater than that measured for model 1.

Some information on the effects of taper and the sign of the sweep angle on the over-all drag characteristics of the configuration at transonic speeds may be obtained by comparison of the results presented in figure 9 for models 4, 6, and 7. Note that the wing area for model 4 was greater than that of models 6 and 7. If the results shown in figure 9 for these models were based on the same wing area, the curve for model 4 would fall almost exactly on the curve for model 7. It is evident that neither taper nor sweepforward appreciably affected the over-all drag during the abrupt drag rise. Beyond the drag rise, however both the configuration having the sweptback tapered wing and that having the sweptforward tapered wing had appreciably higher over-all drags than did the configuration with an untapered, sweptback wing. The higher drags of models 4 and 7 at supersonic speeds were shown previously to occur principally in the drag of the identical body-tail combinations.

Thus, the effect of taper is to replace the favorable interference effect on the body drag of an untapered, sweptback wing located behind the maximum diameter of the body (see reference 3 and the present paper) by a large unfavorable interference effect.

[redacted]

CONCLUDING REMARKS

Free-fall measurements of the transonic drag characteristics of three wing-body combinations - two having untapered, 35° sweptback wings with thickness ratios of 0.09 and 0.12 and one having a 35° sweptback wing of 0.12 thickness ratio and tapered 1.467:1 - are presented herein and are compared with results previously reported for related configurations and with theoretical calculations. The comparison shows the following effects of wing sweep angle, taper, and thickness ratio on the transonic drag characteristics of these wing-body combinations and their component parts:

(1) Either reduction of wing thickness ratio or increase of the sweepback angle resulted in a large reduction of the wing drag and overall drag at supersonic speeds and delayed the occurrence of the drag rise to high Mach numbers.

(2) For the configurations having untapered wings, the drag of the body-tail combination was somewhat increased near the speed of sound by either reduction of wing sweepback or increase in wing thickness ratio but remained lower at supersonic speeds than that of an identical body-tail combination tested without wings.

(3) The drag of the body-tail combination in the presence of either a sweptforward, tapered wing or a sweptback, tapered wing was considerably increased over that of the body-tail combination without wings, the greater part of the increase resulting from the effect of taper. The sign of the sweep angle did not appear to affect the wing drag appreciably.

(4) The wing drag results for the 35° swept wings were not consistent with those predicted by linearized theory for sweptback wings of finite span (NACA TN No. 1319) but correlated satisfactorily with results for unswept airfoils when plotted in the form $\frac{C_D}{\cos^3\Lambda(t/c)^2}$ against $M\sqrt{\cos\Lambda}$. For the 45° sweptback wing the correlation on this basis was also satisfactory except above a Mach number of 1.02. The effect of the presence of the body on the wing drags is to reduce the Mach number at which the abrupt drag rise occurs by an amount approximately equal to the difference between the estimated local Mach number on the body at the wing root and the flight Mach number.

Langley Aeronautical Laboratory
National Advisory Committee for Aeronautics
Langley Field, Va.

REFERENCES

1. Thompson, Jim Rogers, and Mathews, Charles W.: Total Drag of a Body of Fineness Ratio 12 and Its Stabilizing Tail Surfaces Measured during Free Fall at Transonic Speeds. NACA CB No. L6D08, 1946.

2. Mathews, Charles W., and Thompson, Jim Rogers: Free-Fall Measurements at Transonic Velocities of the Drag of a Wing-Body Configuration Consisting of a 45° Swept-Back Wing Mounted Forward of the Maximum Diameter on a Body of Fineness Ratio 12. NACA RM No. L6L26, 1947.

3. Mathews, Charles W., and Thompson, Jim Rogers: Comparison of the Transonic Drag Characteristics of Two Wing-Body Combinations Differing Only in the Location of the 45° Sweptback Wing. NACA RM No. L7I01, 1947.

4. Thompson, Jim Rogers, and Mathews, Charles W.: Drag of Wing-Body Configuration Consisting of a Swept-Forward Tapered Wing Mounted on a Body of Fineness Ratio 12 Measured during Free Fall at Transonic Speeds. NACA RM No. L6L24, 1947.

5. Bailey, F. J., Jr., Mathews, Charles W., and Thompson, Jim Rogers: Drag Measurements at Transonic Speeds on a Freely Falling Body. NACA ACR No. L5E03, 1945.

6. Mathews, C. W., and Thompson, J. R.: Measurements of Static and Total Pressure throughout the Transonic Speed Range As Obtained from an Airspeed Head Mounted on a Freely Falling Body. NACA RM No. L7C04a, 1947.

7. Harmon, Sidney M., and Swanson, Margaret D.: Calculations of the Supersonic Wave Drag of Nonlifting Wings with Arbitrary Sweepback and Aspect Ratio. Wings Swept behind the Mach Lines. NACA TN No. 1319, 1947.

8. Thompson, Jim Rogers, and Mathews, Charles W.: Measurements of the Effects of Thickness Ratio and Aspect Ratio on the Drag of Rectangular-Plan-Form Airfoils at Transonic Speeds. NACA RM No. L7E08, 1947.

9. Lees, Lester: A Discussion of the Application of the Prandtl-Glauert Method to Subsonic Compressible Flow over a Slender Body of Revolution. NACA TN No. 1127, 1946.

[redacted]

TABLE I

COORDINATES OF BODY - MODELS 5, 6, AND 7

[Fineness ratio, 12; nose radius, 0.060 in.]

x (in.)	y (in.)
0.00	0.000
.60	.277
.90	.358
1.50	.514
3.00	.866
6.00	1.446
9.00	1.936
12.00	2.365
18.00	3.112
24.00	3.708
30.00	4.158
36.00	4.489
42.00	4.719
48.00	4.876
54.00	4.971
60.00	5.000
66.00	4.955
72.00	4.828
78.00	4.610
84.00	4.274
90.00	3.754
96.00	3.031
102.00	2.222
108.00	1.350
114.00	.526
120.00	.000

NACA

TABLE II

ESTIMATED MAXIMUM PERCENTAGE UNCERTAINTIES OF DRAG PARAMETERS

Drag parameter \ Mach number	0.90	1.00	1.17
Model 5 (NACA 65-009 wing)			
D/F_p Total	±7.7	±2.4	±0.7
Wing	18.9	2.8	.9
Body and Tail	19.0	8.5	3.2
C_{D_F} Total	10.0	4.4	2.4
Body and Tail	21.2	10.5	4.9
C_D Wing	21.1	4.8	2.7
Model 6 (NACA 65_1-012 wing)			
Drag parameter \ Mach number	0.90	1.00	1.09
D/F_p Total	±1.5	±1.4	±0.7
Wing	9.5	1.9	.9
Tail	25.0	6.6	3.4
Body and Tail	10.5	7.6	4.6
C_{D_F} Total	3.7	3.4	2.5
Body and Tail	12.7	9.6	6.5
C_D Tail	27.0	8.6	5.2
Wing	11.5	3.9	2.8
Model 7 (NACA 65_1-012 wing)			
Drag parameter \ Mach number	0.90	1.00	1.08
D/F_p Total	±1.2	±1.2	±0.7
Wing	6.6	1.8	1.0
Tail	25.0	5.7	3.5
Body and Tail	9.5	6.0	4.0
C_{D_F} Total	3.4	3.2	2.6
Body and Tail	11.7	8.0	5.9
C_D Tail	27.2	7.7	5.4
Wing	8.8	3.8	2.9

[redacted]

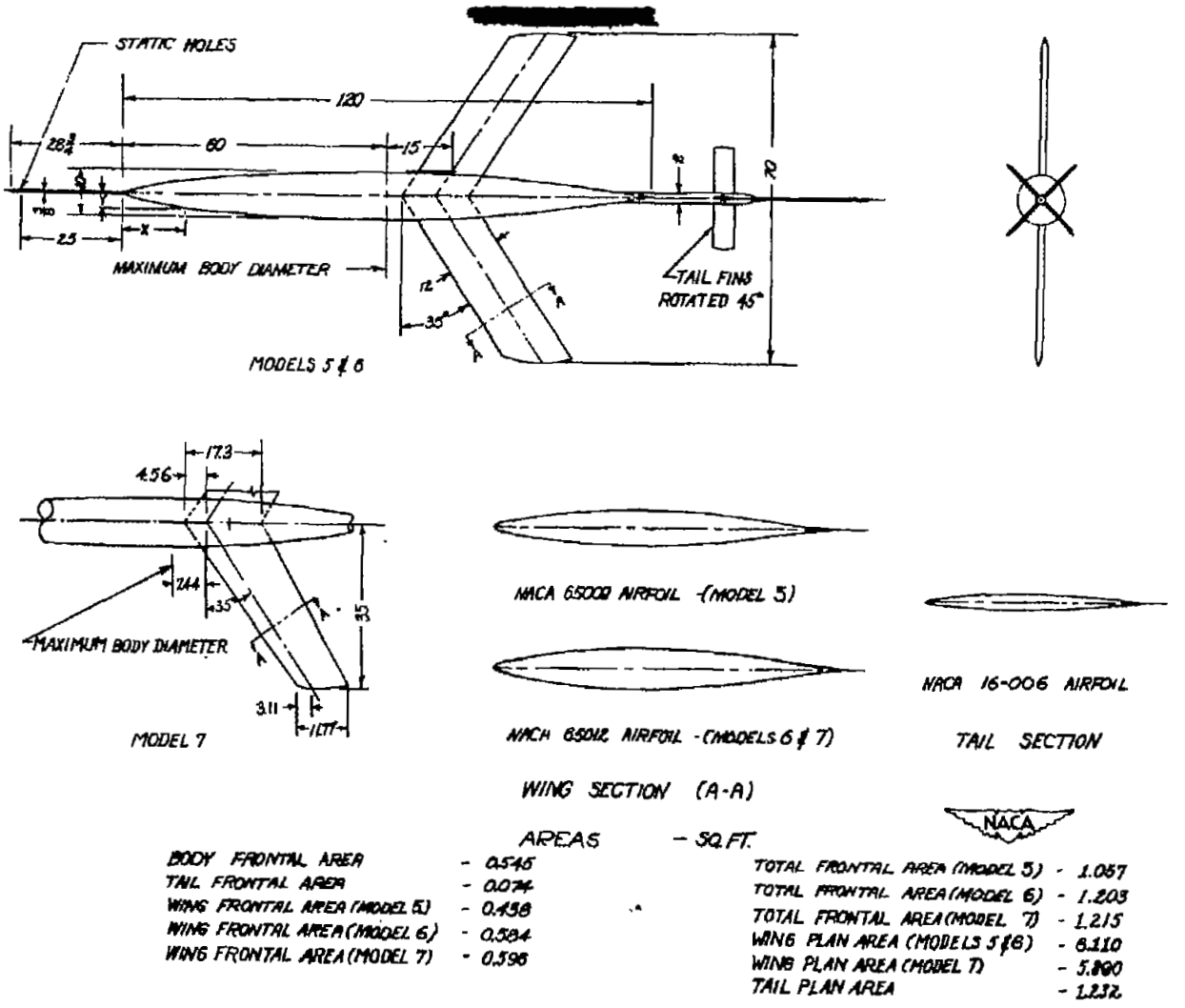

Figure 1.– Details and dimensions of wing-body combinations (models 5, 6, and 7). (All dimensions are in inches.) Body coordinates are given in table I.

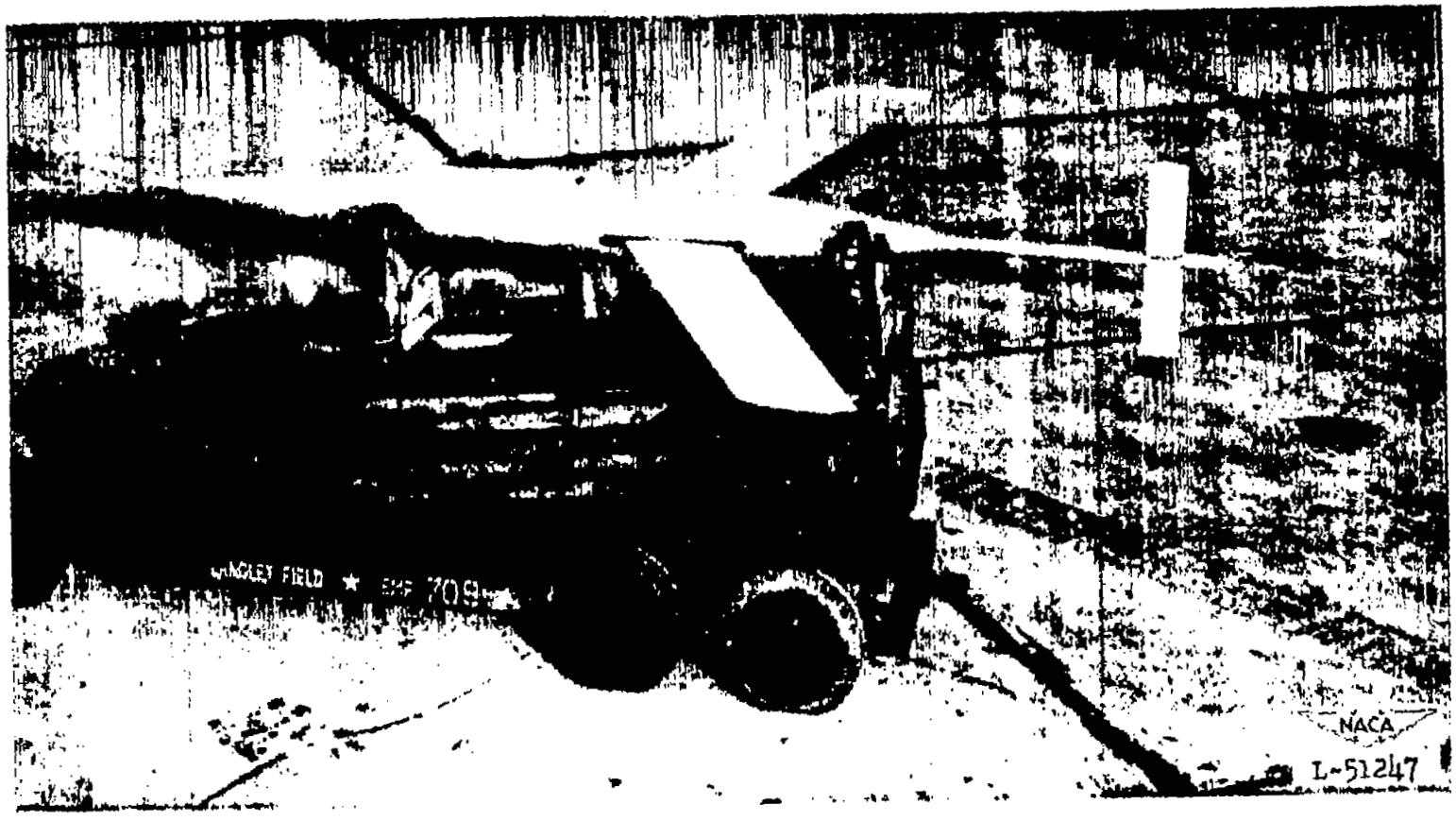

(a) Untapered wing.

Figure 2.- Wing-body combination with 35° sweptback wing located behind the maximum diameter of the body.

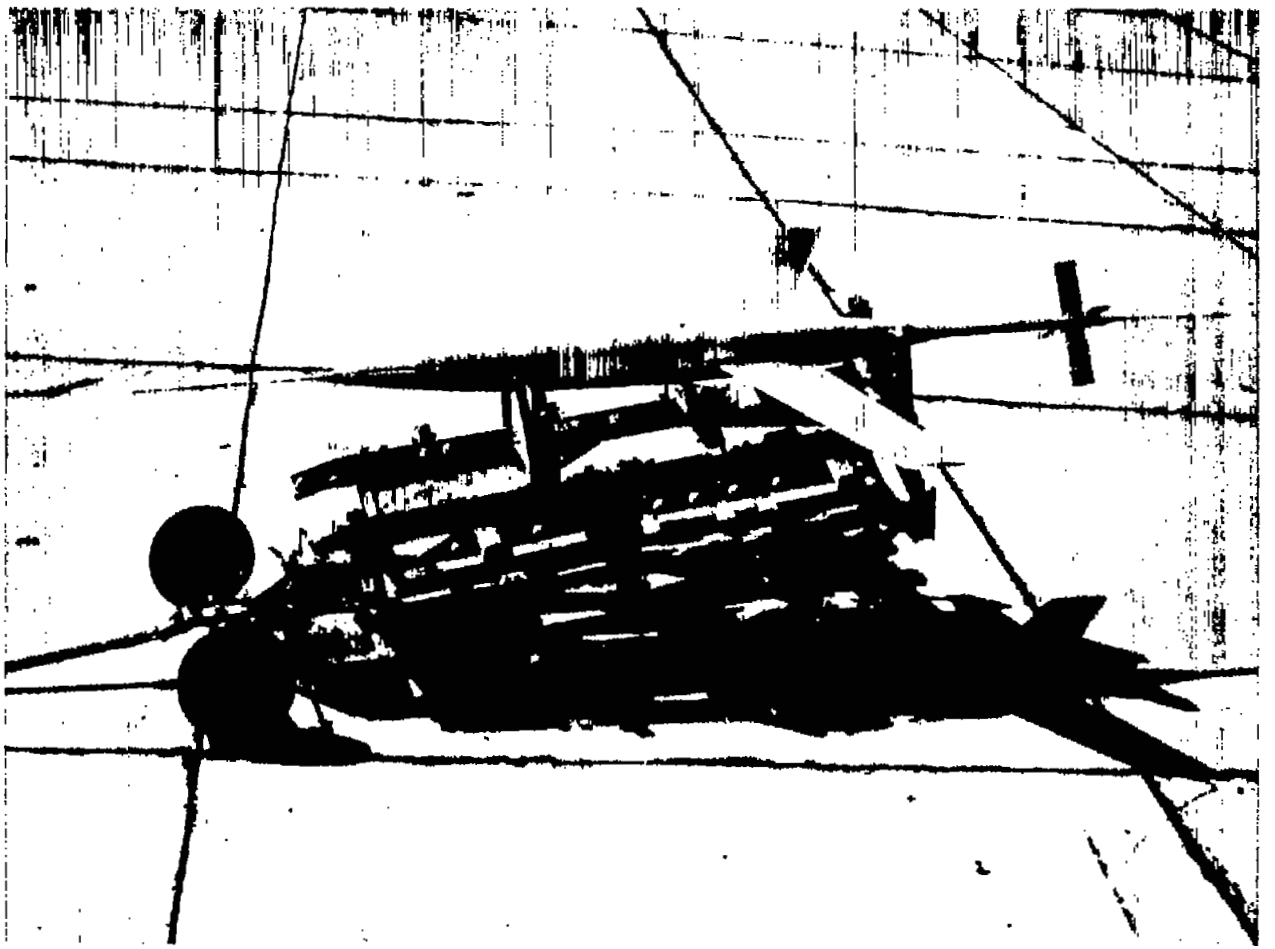

(b) 1.4:1 tapered wing.

NACA L-55769

Figure 2.- Concluded.

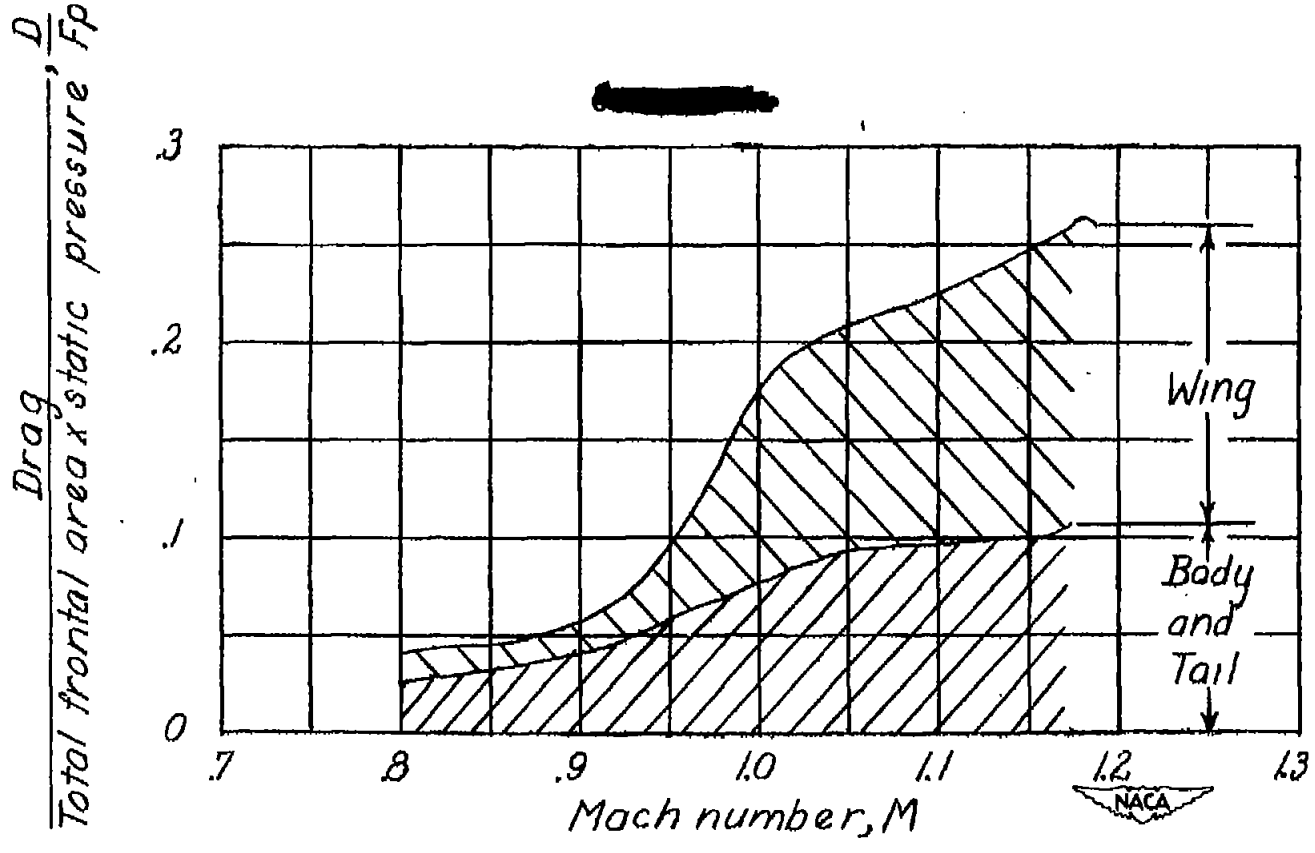

(a) Model 5 (NACA 65-009 untapered wing, 35° sweep).

Figure 3.– Variation of D/F_p ratio with Mach number for models 5 to 7 showing the distribution of the total drag among the component parts.

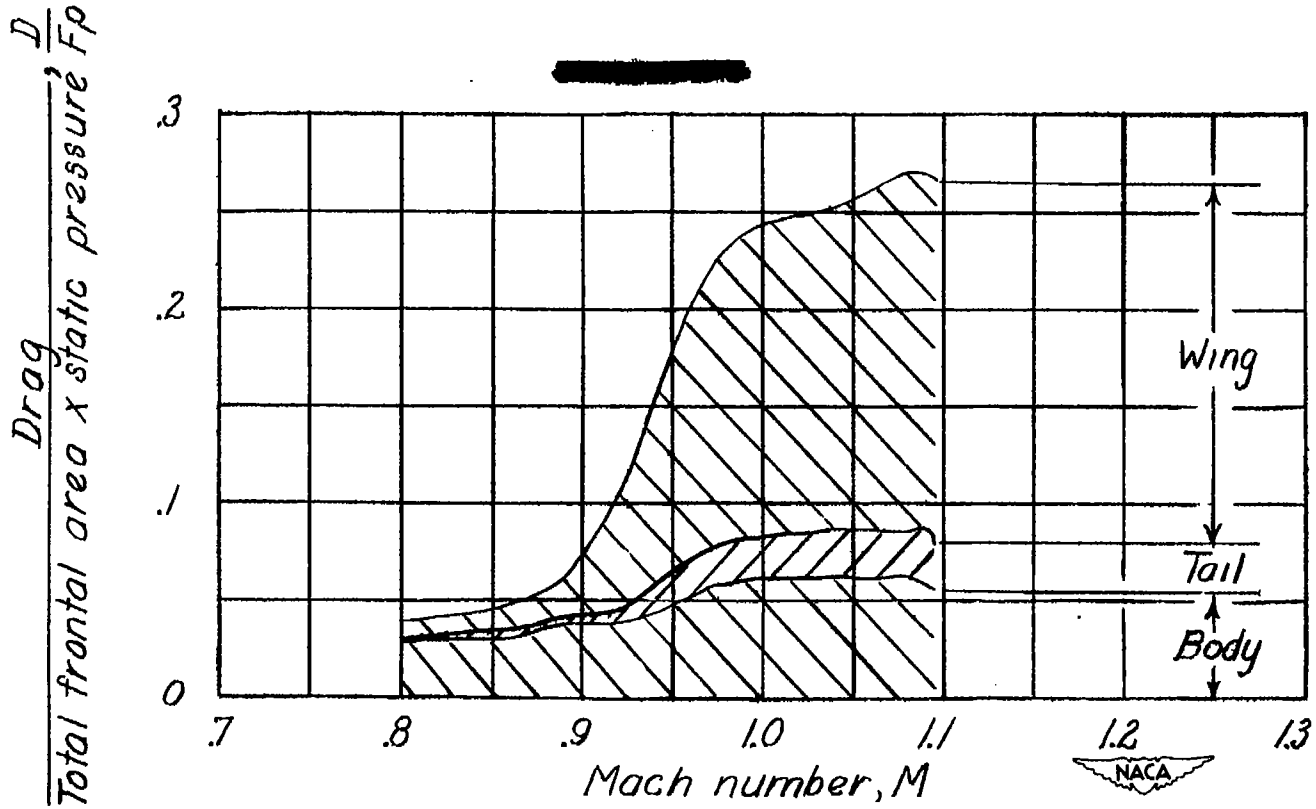

(b) Model 6 (NACA 65_1-012 untapered wing, 35° sweep).

Figure 3.- Continued.

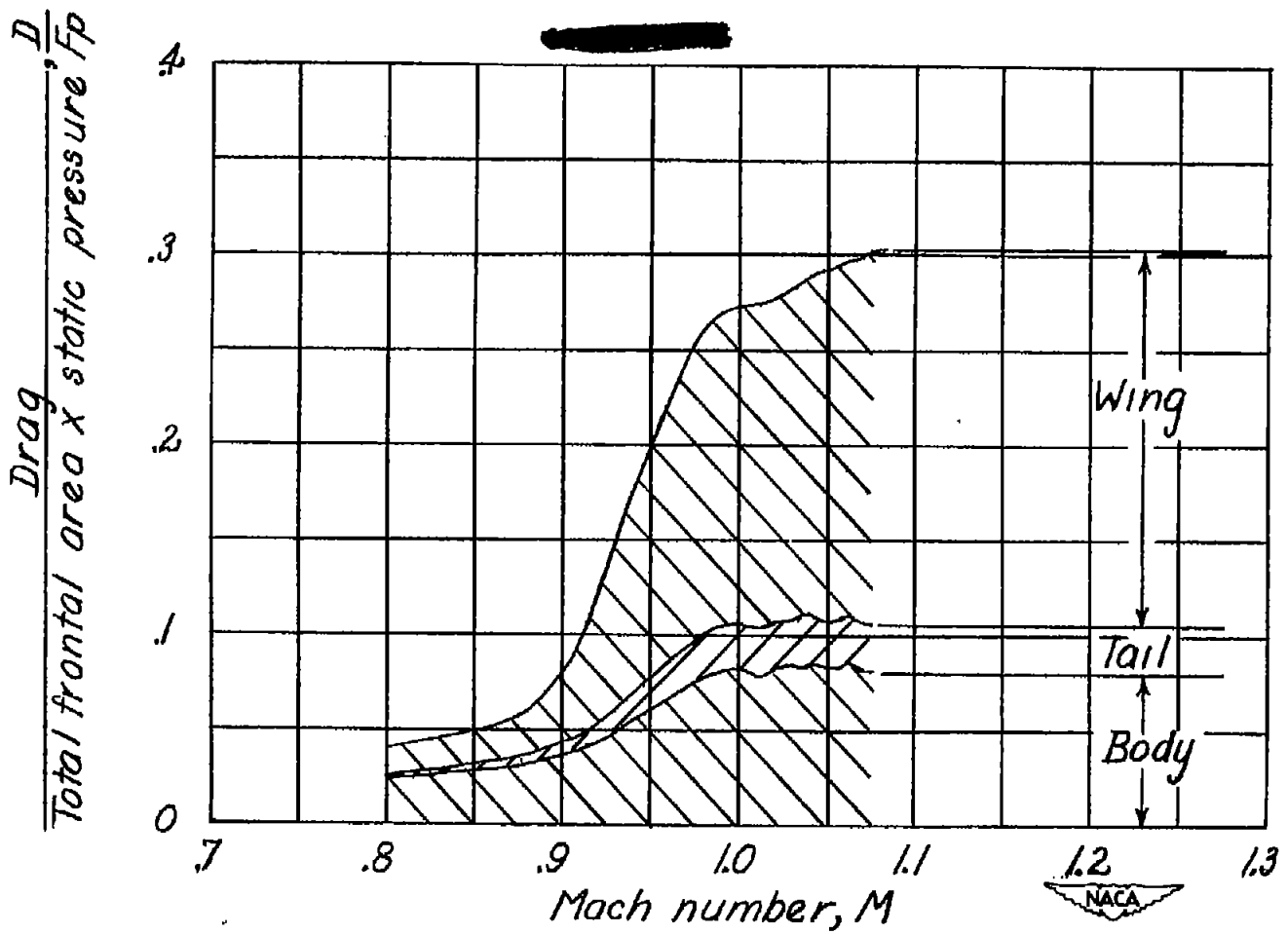

(c) Model 7 (NACA 65_1-012 wing tapered 1.467:1, 35° sweep).

Figure 3.- Concluded.

Model number	5	6	3	–	–	–
Section (NACA)	65-009	65-012	65-009	Circular-arc		
Aspect ratio	4.8	4.8	4.1	4.1	4.1	3.6
Sweep	35	35	45	35	35	45
Taper	1:1	1:1	1:1	1:1	1:1	1:1
Reference	–	–	3	7	7	7

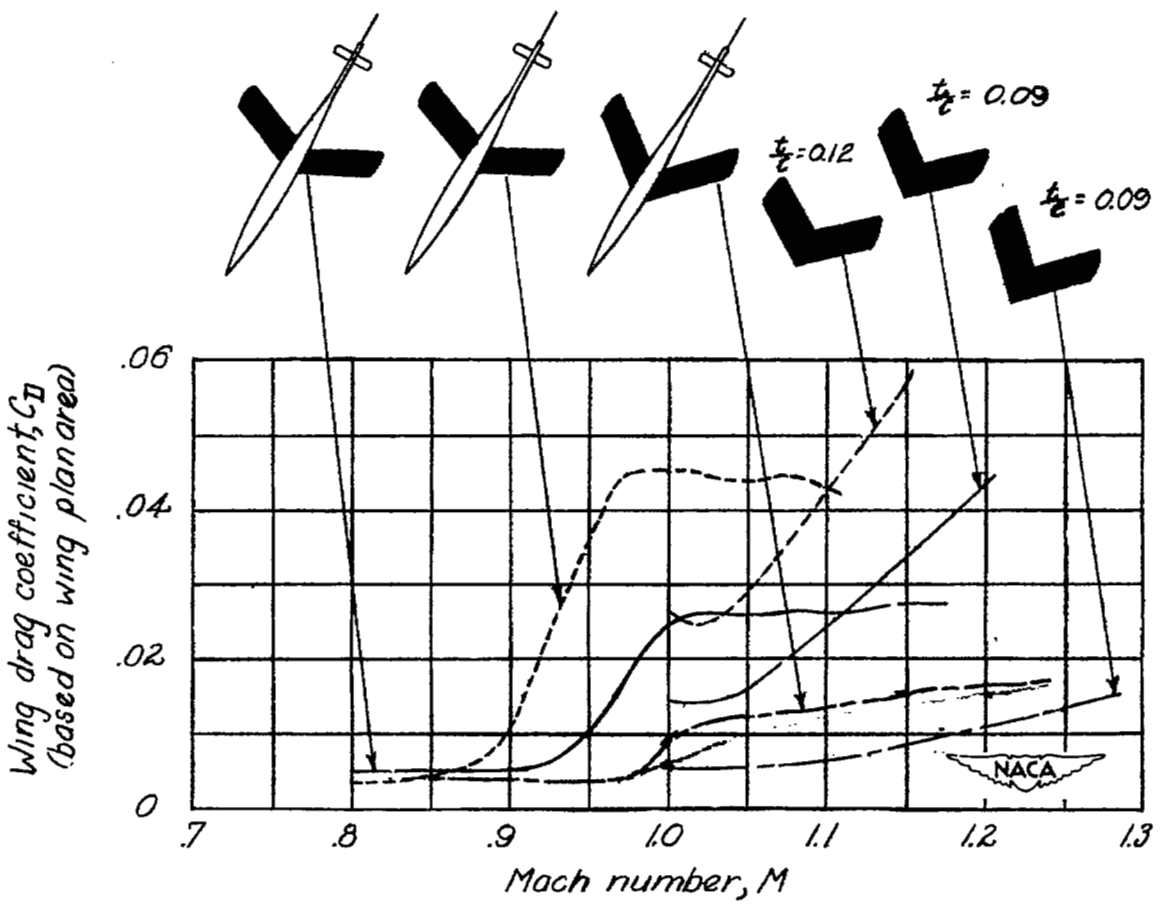

Figure 4.– Comparison of wing drag results for models 5 and 6 with results for related wings. Drag coefficients for the isolated wings were taken from the theoretical results of reference 7 and do not include skin friction.

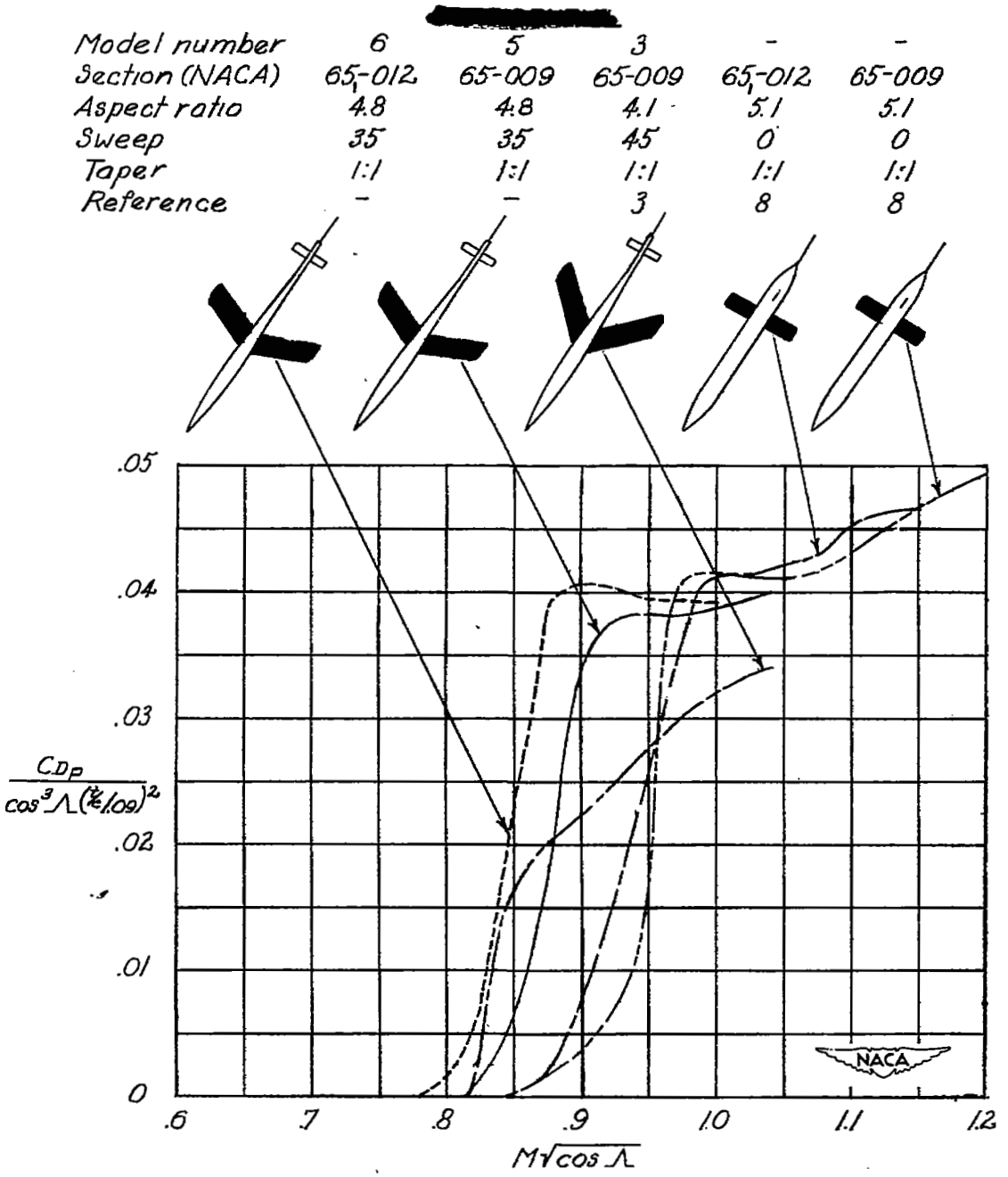

Figure 5.— Correlation of drag results for swept wings located behind the maximum diameter of a fineness-ratio-12 body with results for unswept airfoils tested on cylindrical bodies by use of a modification of infinite-yawed-wing theory. Skin-friction drag coefficient assumed to be 0.005.

Model number	4	7	6
Section (NACA)	65$_1$-012	65$_1$-012	65$_1$-012
Aspect ratio	4.0	4.8	4.8
Sweep	-33.7	32.9	35
Taper	2:1	1.467:1	1:1
Reference	4	-	-

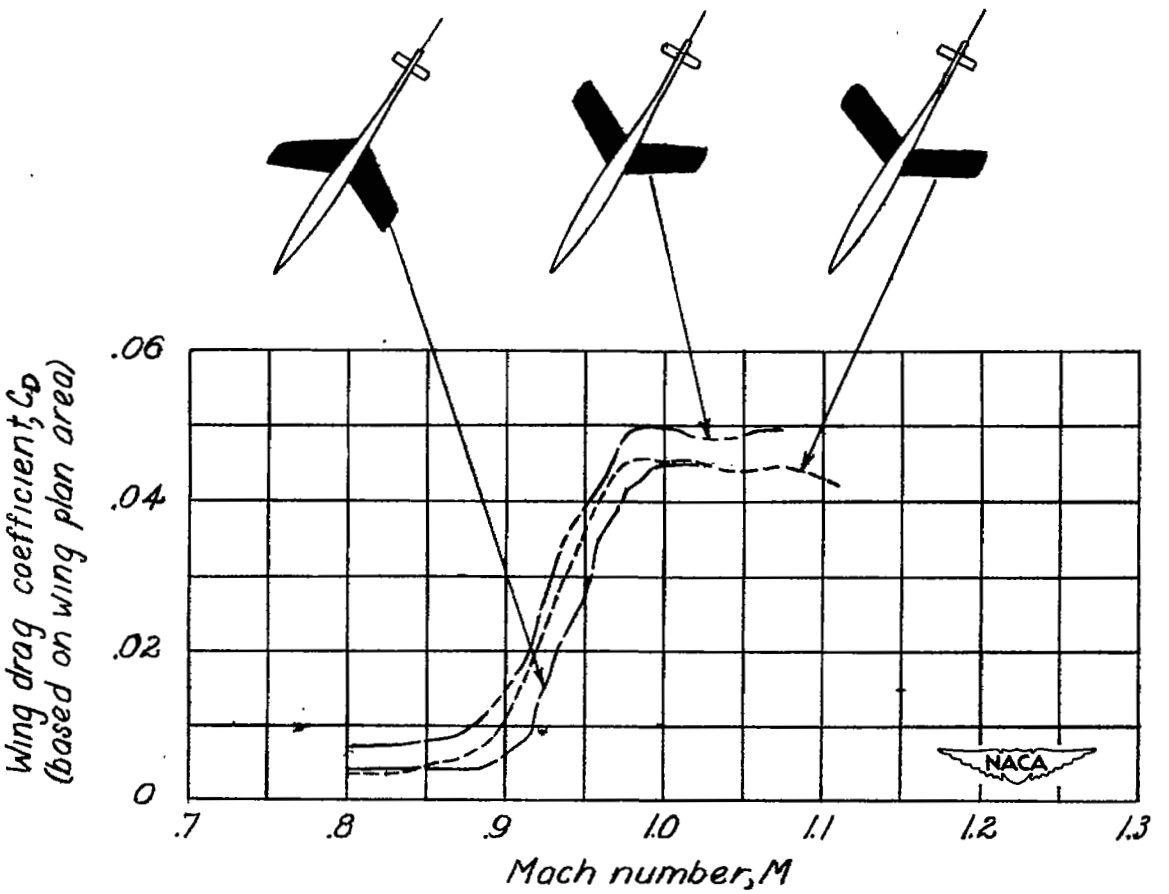

Figure 6.– Comparison of wing drag results for models 4, 6, and 7.

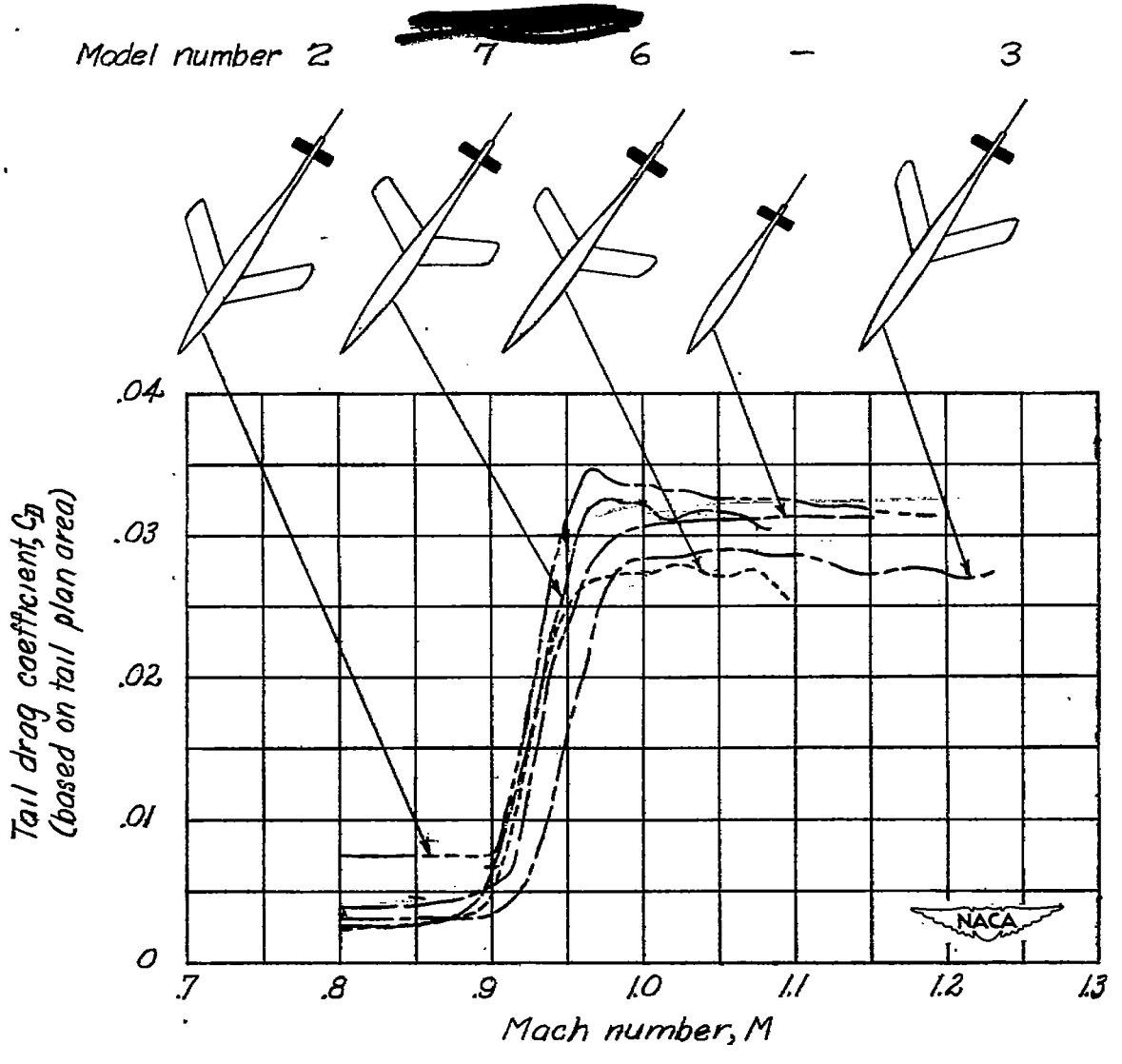

Figure 7.— Comparison of tail drag results for models 6 and 7 with results for identical tails tested on other bodies.

Model number	6	4	7	1	5	3
Section (NACA)	65-012	65-012	65-012	(No	65-009	65-009
Aspect ratio	4.8	4.0	4.8	wing)	4.8	4.1
Sweep	35	-33.7	32.9		35	45
Taper	1:1	2:1	1.467:1		1:1	1:1
Reference		4	-	1	-	3

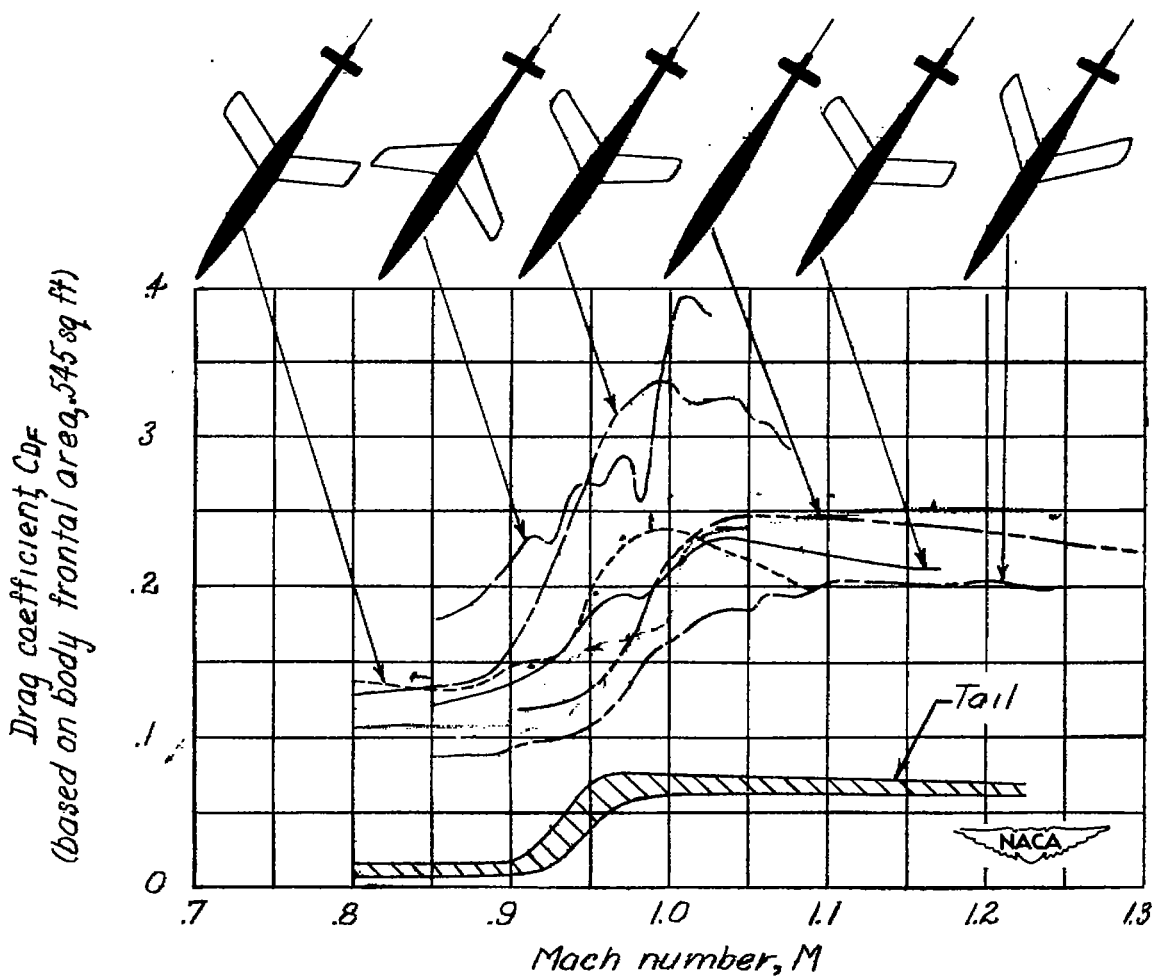

Figure 8.– Effect of wing sweep and thickness on the drag of the body–tail combination. The width of the cross-hatched band corresponds to the spread of the tail drag results of figure 7.

Model number	6	4	7	5	3	1
Section (NACA)	65$_1$-012	65$_1$-012	65$_1$-012	65-009	65-009	(No
Aspect ratio	4.9	4.0	4.8	4.8	4.1	wing)
Sweep	35	-33.7	32.9	35	45	
Taper	1:1	2:1	1.467:1	1:1	1:1	
Wing area, sq.ft.	6.1	8.0	5.9	6.1	7.0	
Reference	-	4	-	-	3	1

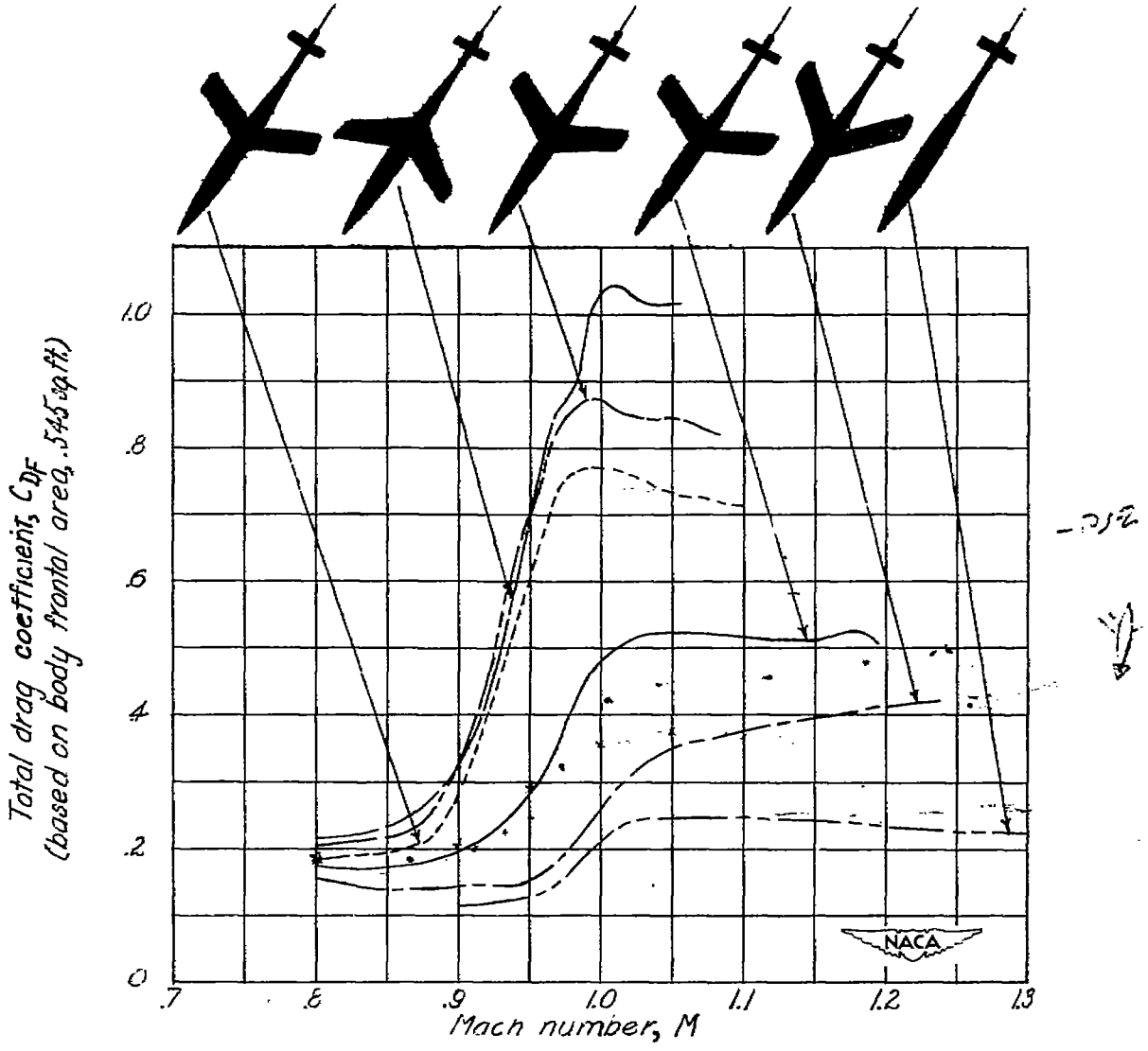

Figure 9.— Comparison of total drag coefficients for models 5 to 7 with results for related configurations. The drag coefficients are based on the body frontal area which is constant for all models.